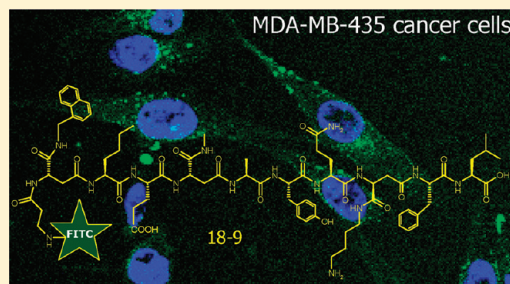


## Proteolytically Stable Cancer Targeting Peptides with High Affinity for Breast Cancer Cells

Rania Soudy,<sup>†</sup> Avneet Gill,<sup>†</sup> Tara Sprules,<sup>‡</sup> Afsaneh Lavasanifar,<sup>†</sup> and Kamaljit Kaur<sup>\*,†</sup><sup>†</sup>Faculty of Pharmacy and Pharmaceutical Sciences, University of Alberta, Edmonton, Alberta, T6G 2N8, Canada<sup>‡</sup>Quebec/Eastern Canada High Field NMR Facility, McGill University, Montreal, Quebec, H3A 2A7, Canada

## Supporting Information

**ABSTRACT:** Cancer cell targeting peptides have emerged as a highly efficient approach for selective delivery of chemotherapeutics and diagnostics to different cancer cells. However, the use of  $\alpha$ -peptides in pharmaceutical applications is hindered by their enzymatic degradation and low bioavailability. Starting with a 10-mer  $\alpha$ -peptide **18** that we developed previously, here we report three novel analogues of **18** that are proteolytically stable and display better (up to 3.5-fold) affinity profiles for breast cancer cells compared to **18**. The design strategy involved replacement of two or three amino acids in the sequence of **18** with D-residues or  $\beta^3$ -amino acids. Such replacement maintained the specificity for cancer cells (MDA-MB-435, MDA-MB-231, and MCF-7) with low affinity for control noncancerous cells (MCF-10A and HUVEC), showed an increase in secondary structure, and rendered the analogues completely stable to human serum and liver homogenate from mice. The three analogues are potentially safe with minimal cellular toxicity and are efficient targeting moieties for specific drug delivery to breast cancer cells. The strategy used here may be adapted to develop peptide analogues that will target other cancer cell types.



## INTRODUCTION

Chemotherapeutic agents are used in conjunction with other treatment options such as surgery, radiation, and hormonal therapy to combat cancer.<sup>1,2</sup> A major hurdle associated with current chemotherapeutic agents is that they enter healthy tissues in the body with indiscriminate cytotoxicity and do not preferentially accumulate at tumor sites.<sup>3,4</sup> To improve the specific uptake of therapeutic agents to cancerous cells in tumors, different strategies have been developed. One of the most effective strategies is to target anticancer drugs preferentially to the tumor site using targeting ligands such as engineered antibodies,<sup>5,6</sup> tumor homing peptides,<sup>7,8</sup> affibodies,<sup>9,10</sup> and aptamers<sup>11</sup> that target specific receptors on particular types of cancer cells. Recently, a number of tumor homing peptides have been reported that specifically target cancer cells and show promising results for tumor targeted drug delivery. Peptides, being smaller than other targeting ligands, have excellent tissue penetration properties and can be easily conjugated to drugs and oligonucleotides by chemical synthesis. Peptides are nearly invisible to the immune system and are not taken up in the reticuloendothelial system like antibodies and so are expected to cause minimal or no side effects to bone marrow, liver, and spleen.<sup>12</sup>

A number of peptides have been identified by peptide phage display for targeting breast cancer cell types.<sup>13–15</sup> One of those is a dodecapeptide identified through phage display by Zhang et al, referred to as peptide p160.<sup>16</sup> Peptide p160 displays high affinity for the human breast cancer cell lines MDA-MB-435 and MCF-7 in vitro with very little affinity for primary

endothelial HUVEC cells.<sup>16–18</sup> Furthermore, in in vivo biodistribution experiments in tumor-bearing mice, p160 showed a higher uptake in tumors than in organs such as heart, liver, lung, and kidney. Relative to the RGD-4C peptide, p160 showed high accumulation in tumor versus normal organs.<sup>18</sup>

Experiments with p160 peptide suggest that a cancer specific receptor is involved in the cellular binding of the peptide.<sup>18</sup> A competitive binding experiment in the presence of increasing concentration of the unlabeled p160 peptide showed reduced uptake of labeled p160 in the MDA-MB-435 cancer cells. In contrast, unspecific competitors such as octreotide and D-p160 (D-isomer) showed no effect on the uptake of the labeled p160. Further, the internalization of the radiolabeled and the FITC-labeled p160 was inhibited in the presence of the unlabeled peptide and was suppressed at 4 °C. Using p160 as a lead peptide, we designed and synthesized a library of 70 peptides on a cellulose membrane. Screening of the library for cancer specific peptides led to the identification of decapeptide **18**, which displayed up to 3-fold higher binding affinity for MDA-MB-435 and MCF-7 cancer cell lines compared to the p160 peptide, with negligible affinity for HUVEC cells.<sup>19</sup> The apparent dissociation constant of peptide **18** for recognizing MDA-MB-435 cells was found to be in the low micromolar range ( $K_d = 42 \mu\text{M}$ ).

Despite the potential of peptide **18** as a potent tumor homing peptide, its applicability would be largely hampered by its instability toward proteases. A fast degradation of p160

Received: June 10, 2011

Published: October 3, 2011

peptide by the serum proteases has been observed.<sup>17,18</sup> The susceptibility of  $\alpha$ -peptides, such as p160 and peptide **18**, to in vivo proteolysis severely diminishes their bioavailability in tissues and organs. This presents a significant hurdle and a major impediment in the development of  $\alpha$ -peptides into clinically useful products.<sup>20</sup> To overcome this, peptides have to be chemically modified so that their blood clearance is minimized in comparison with their rate of uptake at the target sites. The most common strategies used to increase peptide proteolytic stability include introduction of D- or unnatural amino acids and peptide cyclization.<sup>21,22</sup> Introduction of peptidomimetic  $\beta$ -amino acids in an  $\alpha$ -peptide imparts stability against degradation. For instance, mixed  $\alpha/\beta$ -peptides synthesized by replacement of  $\alpha$ - with  $\beta$ -amino acids display enzymatic stability against different proteases compared to the corresponding  $\alpha$ -peptides.<sup>23–28</sup>

The objective of the current study was to develop analogues of cancer targeting peptide **18** to improve proteolytic stability and maintain specific affinity for breast cancer cells. The hypothesis was that peptide **18** can be converted into a proteolytically stable peptide by replacement of a few amino acids while maintaining the secondary structure of the peptide and specific affinity for breast cancer cells. Two approaches were used to develop the analogues. First, a second generation of p160 analogues was created by introduction of single or double substitutions in the peptide **18** sequence to improve specificity for breast cancer cells. Second, proteolytically stable analogues of peptide **18** were explored.

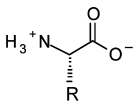
Accordingly, we have designed and synthesized 10 FITC-labeled peptide **18** analogues (Table 1). All the analogues

display high affinity for cancer cells compared to noncancerous cells. Three analogues (**18-4**, **18-9**, and **18-10**) display exceptional resistance to proteolytic degradation in human serum and show higher uptake (up to 3.5-fold) by the breast cancer cell lines MDA-MB-435, MDA-MB-231, MCF-7 compared to peptide **18**. These analogues show low affinity for control (non-cancerous) MCF-10A and HUVEC cells. One of the analogues, **18-4**, consists of two L- to D-amino acid replacements in **18**, whereas the other two (**18-9** and **18-10**) contain three  $\alpha$ - to  $\beta^3$ -amino acid (derived from L-Asp)<sup>29</sup> substitutions. Here we show for the first time that L-Asp can be used as an effective and inexpensive  $\beta$ -amino acid replacement onto which side chain mimics can be placed by making amide analogues on the  $\alpha$ -carboxylate. The analogues maintain a stable secondary structure like the parent peptide **18** and impart no cytotoxicity. This study demonstrates discovery of three novel proteolytically stable breast cancer targeting peptides with potential applicability in anticancer drug delivery and cancer diagnostics.

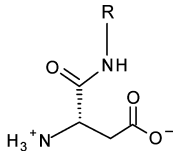
## MATERIALS AND METHODS

**Peptide Synthesis.** Eleven 10-mer peptides (Table 1, **18-1** to **18-10**) were synthesized manually using solid phase peptide synthesis on 2-chlorotrityl chloride resin (0.2 mmol, 1 mmol/g) as described previously.<sup>19,25</sup> The chemical structures of the peptides containing D- or  $\beta$ -amino acids are shown in Figure 1. The first Fmoc-amino acid was coupled using DIPEA for 6 h. Further amino acids were coupled at 2-fold excess using HCTU/HOBt/NMM as activating mixture in DMF. After coupling for 2 h at room temperature, the ninhydrin test<sup>30</sup> was performed to estimate the completeness of the reaction. For mixed  $\alpha/\beta$ -peptide analogues (**18-5** to **18-10**),  $\beta^3$ -amino acids were added to the backbone of the peptide following Fmoc/allyl combined

**Table 1. Primary Amino Acid Sequences and Characterization (Mass Spectrometry and HPLC) of Cancer Targeting Peptides Studied Herein<sup>c</sup>**



$\alpha$ -amino acid



$\beta^3$ -amino acid

Peptide	Amino acid Sequence	[M+H] <sup>+</sup> <sup>a</sup>		Yield (%)	Rt <sup>b</sup> (min)	
		Calcd.	Obsd.		Sol 1	Sol 2
<i><math>\alpha</math>-Peptides</i>						
<b>18</b> (control)	W <b>X</b> EAA <b>Y</b> QR <b>F</b> FL	1367.7	1367.9	70	23.2	29.4
<b>18-1</b>	<b>Y</b> XEAA <b>Y</b> QR <b>F</b> FL	1343.5	1343.1	60	24.5	29.2
<b>18-2</b>	W <b>E</b> EAA <b>Y</b> QR <b>F</b> FL	1383.6	1384.8	70	24.3	29.1
<b>18-3</b>	W <b>L</b> EAA <b>Y</b> QR <b>Y</b> FL	1383.6	1383.5	75	24	29.0
<b>18-4</b>	W <b>x</b> EAA <b>Y</b> Q <b>r</b> FL	1367.7	1367.9	63	23.1	29.3
<i>Mixed <math>\alpha/\beta</math>-Peptides</i>						
<b>18-5</b>	W <b>X</b> EAA <b>Y</b> Q <b>K</b> FL	1454.5	1454.4	45	24.1	29.3
<b>18-6</b>	W <b>X</b> EAA <b>Y</b> QR <b>F</b> FL	1482.1	1483.1	50	24.6	29.4
<b>18-7</b>	W <b>X</b> EAA <b>Y</b> QR <b>F</b> FL	1537.2	1538.2	48	24.9	29.7
<b>18-8</b>	W <b>X</b> EAA <b>Y</b> QR <b>F</b> FL	1538.4	1538.2	51	24.7	29.5
<b>18-9</b>	<b>Z</b> XEAA <b>Y</b> Q <b>K</b> FL	1522.1	1522.6	40	24.9	33.2
<b>18-10</b>	<b>Z</b> XEAA <b>Y</b> Q <b>K</b> FL	1522.1	1522.1	35	24.9	33.1

<sup>a</sup>MALDI-TOF of  $\beta$ -Ala-peptide. <sup>b</sup>RP-HPLC retention time of FITC-labeled peptides. Gradient used on a Vydac C18 analytical column was the following: (solvent 1) 15–50% IPA/water (0.1% TFA) in 35 min with a flow rate of 1 mL/min; (solvent 2) 15–55% ACN/water (0.1% TFA) in 35 min with a flow rate of 1 mL/min. <sup>c</sup>Substitution of amino acids in analogues **18-1** to **18-10** is shown in blue ( $\alpha$ -amino acids) or red ( $\beta$ -amino acids derived from L-Asp). Lower case letters denote D-amino acids. X is Nle, and Z is a  $\beta^3$ -residue with a naphthyl side chain.

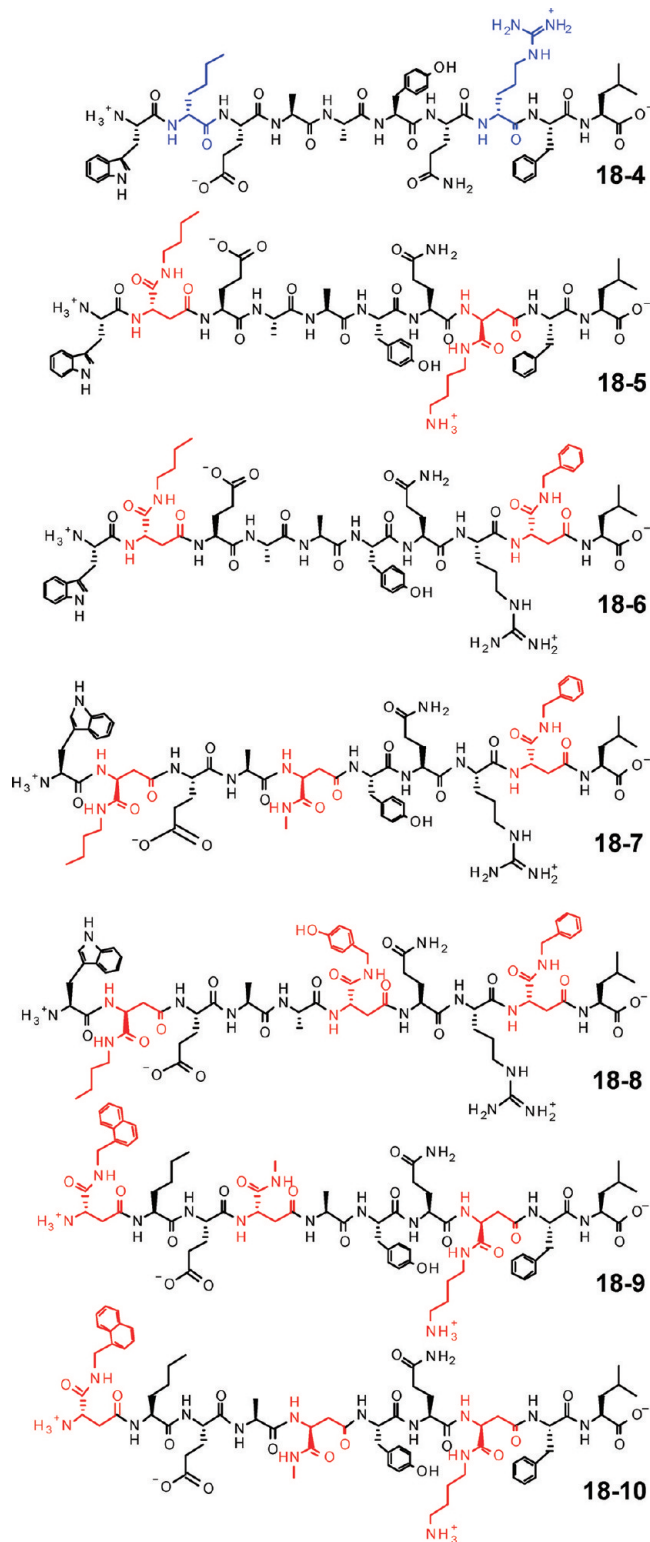


**Figure 1.** Chemical structures of synthesized cancer targeting peptides containing D- or  $\beta$ -amino acids.  $\alpha$ -Amino acids are shown in black (L-amino acids) or blue (D-amino acids), and  $\beta$ -amino acids derived from L-aspartic acid are shown in red.

solid-phase synthesis as previously described.<sup>25,29</sup> Briefly, *N*- $\alpha$ -Fmoc-L-aspartic acid  $\alpha$ -allyl ester was coupled to the growing peptide in DMF using HCTU/HOBt (2 equiv each) and NMM (4.5 equiv) for 2 h at room temp. After coupling, palladium catalyzed deprotection of the side chain allyl from carboxyl group was done under nitrogen using a

mixture of Pd (PPh<sub>3</sub>)<sub>4</sub> (0.08 equiv) and PhSiH<sub>3</sub> (8 equiv) in DCM/DMF (45 min  $\times$  3). Following deallylation, the corresponding amine (RNH<sub>2</sub>, 4 equiv) was coupled using the same coupling reagents as mentioned above for 4 h. Amine side chains used for  $\beta^3$  amino acid syntheses were as follows: methylamine (Sigma) for alanine, *n*-butylamine (Sigma) for norleucine, *tert*-butyl *N*-(4-aminobutyl)-carbamate (TCI-EP) for arginine, benzylamine (Sigma) for phenylalanine, 1-naphthalenemethylamine (Alfa Aesar) for tryptophan, 4-*tert*-butoxybenzylamine (Otava) for tyrosine. Some side chain amine (e.g., methylamine, *n*-butylamine, and 4-*tert*-butoxybenzylamine) couplings required longer times and double coupling. In this case, the concentration of amines should not exceed 2 equiv to prevent cleavage of the Fmoc protecting group before complete coupling. Fmoc groups were removed by treatment with 20% piperidine in DMF, two times each for 7 min. After completion of the synthesis, peptides were cleaved from resin and all protecting groups were removed using cleavage mixture (50:50% TFA/DCM, 5% TIPS) at room temperature for 1 h, followed by washing of the resin with the cleavage reagent twice. The cleaved peptide combined with TFA washes was concentrated by rotary evaporation. Cold Et<sub>2</sub>O (40 mL) was added to precipitate the peptide and then centrifuged. Crude peptides were dissolved in water and purified using reversed-phase HPLC (Varian Prostar 210, U.S.) to obtain pure peptides in 45–70% yield. The purity of the peptides was confirmed by HPLC and MALDI-TOF mass spectrometry (Supporting Information Figure S3). The purity of the peptides was verified to be greater than 95% by RP-HPLC. The HPLC analysis and mass spectrometric data of the peptides are summarized in Table S1. All the peptides were labeled with fluorescein 5-isothiocyanate (5-FITC) through their N-terminus via a  $\beta$ -alanine spacer. The stepwise procedure for FITC conjugation to peptide 18 is shown in Figure S1 (Supporting Information). FITC- $\beta$ -ala-peptides (or FITC-peptides) were verified to be greater than 95% pure by RP-HPLC (Figure S2).

**Cell Culture.** All cancer cell lines and human mammary epithelial cell line MCF-10A were purchased from the American Type Culture Collection (ATCC) and additives were from Invitrogen. Human breast cancer cell line MDA-MB-435 was cultured in RPMI-1640 medium supplemented with 10% FBS, 100 IU/mL penicillin and 100 IU/mL streptomycin, whereas MCF-7 and MDA-231 were cultured in DMEM medium containing 10% FBS, 100 IU/mL penicillin, and 100 IU/mL streptomycin. Human mammary epithelial cell line (MCF-10A) was cultured in minimal essential growth medium MEGM (Lonza, Cedarlane) supplemented with the same additives as before. Human umbilical vein endothelial cells (HUVEC), a kind gift from the laboratory of Sandra Davidge, University of Alberta, Canada, were cultivated using endothelial cell growth medium EGM, (Lonza, Cedarlane) containing 20% FBS, 2 mmol/L glutamine, 100 IU/mL penicillin, 100 IU/mL streptomycin, and 2 ng/mL basic fibroblast growth factor (Roche Diagnostics, Mannheim, Germany). All cell lines were cultivated at 37 °C in a 5% CO<sub>2</sub>–95% O<sub>2</sub> incubator, and growth media were replaced every 48 h.

**Cellular Uptake by Flow Cytometry.** The cellular uptake of the synthesized analogues (18-1 to 18-10) was evaluated against three human breast cancer cell lines (MDA-MB-435, MCF-7, and MDA-MB-231) and two noncancerous cell lines (MCF-10A and HUVEC) using a flow cytometer (Becton-Dickinson Facsfort). Cells were grown in T-75 culture flasks containing medium supplemented with FBS and antibiotics until 80% confluence. After washing twice with PBS, cells were detached from the surface by incubation with trypsin solution at 37 °C. Cells were centrifuged at 500g for 5 min, resuspended in medium, counted by hemocytometer, and diluted to 10<sup>3</sup> cells/mL with medium. Next, they were seeded in a six-well tissue culture plate at a density of 10<sup>6</sup> in 3 mL of culture medium at 37 °C for 24 h. The following day, cells were washed by PBS and incubated in serum free medium containing FITC-labeled peptides at 10<sup>-5</sup> mol/L for 30 min at 37 °C. Then the cells were washed 3 times with PBS, trypsinized to remove any surface bound peptides, and centrifuged at 500g for 5 min. The pellets were resuspended in FACS solution (10% FBS in PBS), and flow cytometry was performed. A total of 10 000 events were collected monitoring fluorescein 5-isothiocyanate (5-FITC). The

autofluorescence of the cells only without treatment was measured to differentiate between the peptide-bound labeled cells and autofluorescence of unlabeled cells. Fluorescence up to the measured intersect was called autofluorescence and represented the cutoff point value. Cells in which fluorescence was higher than that value were considered labeled with 5-FITC. Competitive binding assays were performed using MDA-MB-435 cancer cell line with FITC-18-4 and FITC-18-9 in the presence of 50-fold excess of unlabeled 18-4 and 18-9, respectively. After incubation for 30 min at 37 °C, the cells were washed with ice cold PBS. Thereafter, FACS analysis was performed as described above. All experiments for binding were repeated 2–3 times.

**Fluorescence Microscopy.** MDA-MB-435 or HUVEC cells (50 000) were cultured on the top of a coverslip at 37 °C for 24 h. The medium was removed and replaced with fresh serum free medium (1 mL) containing FITC-labeled peptides (18-4, 18-9) at  $10^{-5}$  mol/L. The cells were incubated with the peptides for 30 min at 37 °C. After incubation, the medium was removed and the cells were washed with serum free medium ( $3 \times 2$  mL). The cells were fixed on ice with 2% formaldehyde for 20 min. The formaldehyde was removed by washing with medium (3 times). The coverslips were put on slides containing one drop of DAPI-Antifade (Molecular Probes) to stain the nucleus. The cells were imaged under the fluorescence microscope (Zeiss) using green and blue filters with 20 $\times$  magnification. The samples prepared for fluorescence microscopy were also used for visualization by confocal microscopy to confirm internalization. Confocal laser scanning microscopy was performed with a Carl Zeiss inverted confocal microscope (Zeiss 510 LSMNLO, Jena, Germany) with a 40 $\times$  oil immersion lens. Confocal stacks were processed using the Carl Zeiss LSM 5 Image software, which also operates the confocal microscope.

**Serum Stability.** The proteolytic stability of selected peptides (18, 18-4, 18-9, and 18-10) in the presence of human serum was evaluated using HPLC analysis. Human serum (250  $\mu$ L) was added to RPMI medium (650  $\mu$ L) in 1.5 mL Eppendorf tube to mimic biological system. The temperature was equilibrated at  $37 \pm 1$  °C for 15 min before adding 100  $\mu$ L of peptide stock solution (1 mM solution in 100% sterile water). The initial time was recorded, and at known time intervals (0, 0.5, 1, 5, and 24 h) an aliquot of reaction solution (100  $\mu$ L) was removed and added to methanol (200  $\mu$ L) for precipitation of serum proteins present in the human serum. The cloudy solution produced was cooled to 4 °C for 15 min and then spun at 500g for 15 min to pellet the serum proteins. The supernatant (50  $\mu$ L) was injected onto a RP-HPLC Vydac C18 column using an autoinjector to eliminate manual injection error. A linear gradient from 12% to 100% IPA/water in 35 min with a flow rate of 1.5 mL/min was used, and the absorbance of the eluting peaks was detected at 214 nm. The concentration of peptides and degradable products was measured by integrating the area under the curve and their identity was confirmed using MALDI-TOF mass spectrometry.

**In Vitro Metabolic Stability.** The in vitro metabolic stability was determined by incubating the peptides with liver homogenate. The liver homogenate was prepared as described previously.<sup>31</sup> Briefly, liver was collected from male CD-1 mice. After the sample was cleaned and washed in ice-cold HEPES buffer (pH 7.4), approximately 0.98 g was transferred to a 50 mL centrifugation tube. Ice-cold HEPES buffer (5 mL) was added, and the organ was homogenized with an Ultra-Turrax (IKA, Staufen, Germany) for 1 min on ice. The homogenate was shaken and subsequently centrifuged at 14 000 rpm for 20 min at 4 °C. Aliquots of the supernatant were transferred into microtubes and stored at  $-80$  °C until use. Before use, the protein content of each homogenate was determined using bicinchoninic acid protein assay (BCA) to generate a stock solution with a protein concentration of 14.7 mg/mL by dilution with HEPES buffer.

For the metabolic stability of the peptides, an aliquot (100  $\mu$ L) from the peptide stock solutions (18-4, 18-9, and 18-10) prepared in 5% ACN/water mixture (1 mM) was added to 900  $\mu$ L of liver extract (200  $\mu$ L of homogenate, 700  $\mu$ L of RPMI medium, pH 7.4, 2.94 mg of protein in total). The mixture was incubated at 37 °C while shaking, and an aliquot (100  $\mu$ L) was taken out at regular time intervals. The enzymatic reaction was stopped by mixing the sample with

methanol (300  $\mu$ L). This also allowed precipitation of proteins, after which the samples were cooled at 0 °C for 30 min. Thereafter, centrifugation at 14 000 rpm for 10 min yielded a clear supernatant, which was analyzed by reversed-phase HPLC on Vydac C18 column with UV detection at 220 nm wavelength. Cleavage products were separated by analytical reversed phase HPLC using 15–55% IPA/water over 35 min and analyzed by MALDI-ToF mass spectrometry. Blank solutions and the control  $\alpha$ -peptide (peptide 18) were similarly treated for comparison. The percent of hydrolysis was determined from the integration of “area under the curve” of the peaks.

**NMR Spectroscopy.** NMR samples of synthetic peptide p160 (VPWXEPAYQRFL) were prepared in water (90% H<sub>2</sub>O/10% D<sub>2</sub>O or 100% D<sub>2</sub>O) or TFE (100% CF<sub>3</sub>CD<sub>2</sub>OH or 100% CF<sub>3</sub>CD<sub>2</sub>OD) (Cambridge Isotope Laboratories, Inc.). Samples of 18 were prepared in a mixture of TFE and water (80% CF<sub>3</sub>CD<sub>2</sub>OH/20% H<sub>2</sub>O or 80% CF<sub>3</sub>CD<sub>2</sub>OD/20% D<sub>2</sub>O). Spectra were recorded at 15 °C. The complete chemical shift assignments for p160 and 18 are listed in Table S1. 2D TOCSY (60 ms mixing time), COSY, ROESY (mixing time 200 ms), and NOESY (mixing time 100, 200, and 300 ms) spectra were recorded on Varian INOVA 500 MHz spectrometer equipped with an HCN cold probe and pulsed-field gradients. Upper distance restraints for p160 structure calculations in TFE were obtained from 200 ms mixing time 2D [1H,1H]-NOESY data recorded at 500 MHz (amide region) and 800 MHz (aliphatic and aromatic regions). Upper distance restraints for p160 structure calculations in H<sub>2</sub>O were obtained from 200 ms mixing time 2D [1H,1H]-ROESY spectra recorded at 500 MHz. Upper distance restraints for 18 structure calculations were obtained from 200 ms mixing time 2D [1H,1H]-NOESYs recorded at 500 MHz. Calculations of the complete three-dimensional structures were performed with the program CYANA, version 2.1.<sup>32</sup> Input data and structure calculation statistics are summarized in Tables S3 and S4. The final calculation was started with 100 randomized conformers to converge to the final conformation. The 20 lowest energy CYANA conformers were used to represent the NMR structure of the peptides.

**CD Spectroscopy.** The circular dichroism (CD) measurements were made on Olis CD spectrometer (GA, U.S.) at 25 °C in a thermally controlled quartz cell with a 0.02 cm path length over 190–260 nm. The samples were prepared by dissolving the peptides in 90% TFE/water mixture containing 0.05% TFA. The final peptide concentration for the CD measurements was 200  $\mu$ M. Data were collected every 0.05 nm and were the average of eight scans. The bandwidth was set at 1.0 nm and the sensitivity at 50 mdeg. The response time was 0.25 s. In all cases, baseline scans of aqueous buffer were subtracted from the experimental readings. The CD data were normalized and expressed in terms of mean residue ellipticity (deg cm<sup>2</sup> dmol<sup>-1</sup>).

**Cytotoxicity.** The cytotoxicity of peptide analogues 18-4, 18-9, and 18-10 was tested by measuring the cell growth inhibition using MTT assay.<sup>33</sup> Breast cancer human cells MDA-MB-435 were seeded in 96-well plates (Corning Inc., MA, U.S.) at  $1 \times 10^4$  cells/well per 200  $\mu$ L of RPMI serum free medium supplemented with antibiotics (100 IU/mL penicillin, 100 IU/mL streptomycin) and incubated at 37 °C in 5% CO<sub>2</sub> atmosphere. After 24 h, the cells were treated with different concentrations of the peptides (1–100  $\mu$ M) prepared in sterile water and incubated for 48 h. Doxorubicin was used as a positive control, and the untreated cells were used as a negative control. The culture medium was discarded and replaced with 200  $\mu$ L of MTT solution (5 mg/mL medium), and cells were incubated for another 3.5 h. All experiments were done in triplicate, and the data in the form of the mean are presented. Following incubation, the medium was sucked out, and the purple formazan product precipitated in each well was solubilized in DMSO (150  $\mu$ L). After gentle shaking for 10 min at room temperature, absorbance was measured at 570 nm using a VersaMax microtiter reader (Molecular Devices, Sunnyvale, CA, U.S.) with a reference wavelength of 650 nm. The percentage cell viability was expressed as the absorbance ratio of cells treated with peptides to untreated cells dissolved in complete medium.

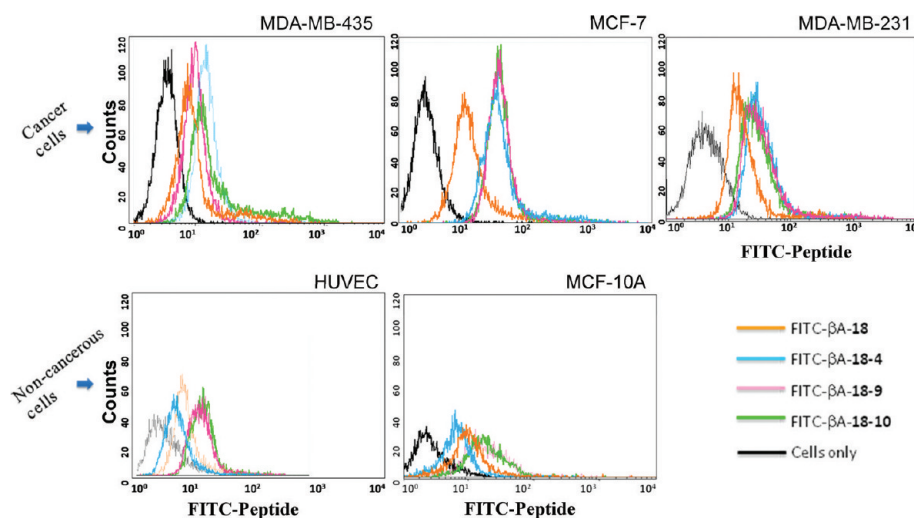


**Figure 2.** Peptide uptake by the cancer cells (top row) MDA-MB-435, MCF-7, and MDA-MB-231 and the control cells (bottom row) HUVEC and MCF-10A measured by flow cytometry. The peptides ( $10^{-5}$  mol/L) FITC-18 (orange), FITC-18-4 (blue), FITC-18-9 (pink), and FITC-18-10 (green) were incubated with the cells for 30 min at 37 °C. Autofluorescence of the cells is shown in black.

## RESULTS

**Design of Peptide 18 Analogues.** Peptide 18 is a linear 10-mer peptide with a net charge of zero that shows high binding affinity to breast cancer cells compared to non-cancerous cells in vitro.<sup>19</sup> In our earlier experiments, 18 was identified through screening of a cellulose membrane-bound peptide array library against cancer cells. The peptide array library was based on a cancer targeting dodecapeptide, p160.<sup>16,19</sup> Deletion of the two N-terminal residues (Val-Pro) of p160 and one Pro → Ala substitution yield decapeptide 18 (Figure 1). Using peptide 18 as a starting point, here we have designed 10 analogues of 18 for selective binding to breast cancer cells. The synthesis of the peptides was done on solid phase as described in the methods section (also see Figure S1). The mass spectrometry data and the HPLC elution time of the peptides are listed in Table 1.

First, three  $\alpha$ -peptide sequences (18-1 to 18-3) were designed to introduce one or more substitution(s) in 18, such as Trp1 → Tyr1, Nle2 → Glu2 or Leu2, and Phe9 → Tyr9, based on the results of our initial peptide array (based on p160) screening.<sup>19</sup> Next, in peptide analogue 18-4, two residues, Nle2 and Arg8, were substituted with D-amino acids to enhance proteolytic stability as well as increase binding affinity to cancer cells. These residues have been identified as the labile sites in the peptide by Askoxyakis and co-workers.<sup>17</sup>

Finally, a number of mixed  $\alpha/\beta$ -peptides (18-5 to 18-10, Figure 1) were designed to improve the proteolytic stability of the lead peptide 18. Analogues 18-5 and 18-6 contain substitution of two labile residues with  $\beta^3$ -amino acids.  $\alpha/\beta$ -Peptides 18-7 to 18-10 each contain three  $\alpha$  to  $\beta^3$  replacements to maximize resistance to proteolysis. These analogues were fabricated following a sequence based design strategy reported by Horne et al.<sup>23,24,34</sup> Here  $\alpha$  and  $\beta$  amino acid residues were distributed in a repeating heptad pattern ( $\alpha\alpha\beta\alpha\alpha\beta$ ) that yields  $\beta$ -residues along one side of the helix.<sup>34</sup> The replacement sites in these four analogues were selected to sample different positions in the heptad repeat. The  $\beta^3$ -amino acids used in this study were derived from L-aspartic acid.<sup>29</sup>

**In Vitro Cell Binding Assays.** The binding of the peptide analogues to different mammalian cell lines was compared to the lead peptide 18 using flow cytometry. FITC-labeled

peptides (18, 18-1 to 18-10) were screened for specific binding to three breast cancer cell lines, namely, MDA-MB-435, MDA-MB-231, and MCF-7, and two noncancerous cell lines, MCF-10A and HUVEC. The results show that all 10 analogues display significant binding to the three breast cancer cell lines, as evidenced by the increase in the percentage of fluorescently labeled positive cells, relative to the untreated cells ( $40\text{--}100\% \pm 10$  for the treated groups and 1% for untreated groups) (Figure S4, Supporting Information). The uptake pattern of all the peptides was similar for the three cancer cell lines with slightly higher uptake for MCF-7 at the concentrations tested. This is in agreement with previous studies that showed that p160 has 7-fold higher binding to MCF-7 compared to MDA-MB-435.<sup>18</sup> Among all the peptides evaluated, peptides 18-4, 18-9, and 18-10 showed the highest binding to the cancer cells (Figure 2).

By comparison of the binding affinity of  $\alpha$ -peptide analogues (18-1 to 18-4) and peptide 18 to cancer cells, it was found that the hydrophobic and/or aromatic substitutions (Trp1 → Tyr1, Nle2 → Leu2, and Phe9 → Tyr9) were more tolerated than the charged amino acid substitution (Nle2 → Glu2). For instance, peptides 18-1 and 18-3 with aromatic or hydrophobic substitutions displayed equal or slightly higher binding affinity ( $\geq 1.5$ -fold), whereas 18-2 with Nle2Glu substitution showed a 3 order of magnitude decrease in binding. The percentage increase in fluorescence (of 18-2 incubated with cells) compared to cells only was  $14 \pm 3\%$ ,  $60 \pm 5\%$ , and  $33 \pm 8\%$  for MDA-MB-435, MCF7, and MDA-MB-231 cells, respectively. Peptide 18 has an average of  $74 \pm 10\%$  increase in fluorescence for the three cell lines. This correlates with our previous observation where a p160 analogue with Phe9Lys charged substitution showed a marked decrease in binding with respect to the parent peptide.<sup>25</sup> In addition, the overall charge for 18-2 is  $-1$  which may also hinder its interaction with the negatively charged surface of the cancer cells.<sup>35</sup> Peptide 18-4, with D-amino acid substitutions at Nle2 and Arg8, was well tolerated and showed up to 3.5-fold increase in peptide affinity to cancer cell lines. As shown in Figure 2, the mean fluorescence intensities of 18 and 18-4, respectively, were  $10 \pm 2$  and  $35 \pm 2$  when incubated with MDA-MB-435,  $22 \pm 2$  and  $68 \pm 2$  with MCF-7, and  $16 \pm 2$  and  $45 \pm 2$  when

incubated with MDA-MB-231 cells. In earlier studies D-p160 with all amino acids replaced with the D-isoforms showed no uptake by the cancer cells and was used as a negative control peptide.<sup>18</sup> The results presented here, however, suggest that the configuration of the two amino acids most likely did not alter the interaction with the receptor. In general, these results reflect that hydrophobic substitutions are beneficial and such interactions increase specific binding of the peptide to the cancer cell.

Mixed  $\alpha/\beta$ -peptide analogues (18-5 to 18-10) with two or three  $\beta$ -amino acid substitutions and variation in the position of the  $\beta$ -residues were also well tolerated. Peptides 18-5, 18-6, 18-7, and 18-8 displayed similar affinity to cancer cells, whereas 18-9 and 18-10 showed a marked increase ( $\sim 3$ -fold) in binding to cancer cells, compared to the parent peptide 18 (Figures S4 and 2). Peptides 18-9 and 18-10 each have three  $\alpha \rightarrow \beta^3$ -amino acid substitutions. The polarity of the side chains was maintained; namely, Trp1 was replaced with a  $\beta^3$ -amino acid with a naphthyl side chain, Ala4 or Ala5 was replaced with methyl, and Arg9 was substituted with a  $\beta^3$ -amino acid with a butylamine side chain. These substitutions led to a slight increase in hydrophobicity of the peptide as observed from the increase in the HPLC retention time of the peptide (Table S1). Previously, Askoxylakis et al. also reported a similar observation where replacement of Ala7 with  $\beta$ -alanine in p160 resulted in a more than 2-fold increase in binding to WAC 2 cells when compared to the native p160.<sup>17</sup>

On the basis of the initial screening results for peptide uptake by cancer cells, three peptides 18-4, 18-9, and 18-10 were selected for further study. The binding affinity and specificity of the selected peptides were evaluated against noncancerous cell lines MCF-10A and HUVEC. MCF-10A cells are derived from human fibrocystic mammary tissue, whereas HUVEC endothelial cells were isolated from normal human umbilical vein. The three peptides displayed significantly lower binding to the control cells versus strong preferential binding to breast cancer cells after 30 min of incubation (Figures S4 and 2). The percent increase in fluorescence (relative to the untreated cells) was  $36 \pm 2\%$ ,  $50 \pm 3\%$ , and  $55 \pm 3\%$  for MCF-10A cells and  $12 \pm 1\%$ ,  $30 \pm 5\%$ , and  $35 \pm 4\%$  for HUVEC when incubated with peptides 18-4, 18-9, and 18-10, respectively. These peptides showed 85–100% increase in fluorescence when incubated with cancer cells showing that peptides bind preferentially to cancer cells. It is also observed that the peptides have relatively higher binding to MCF-10A compared to HUVEC, and this is most likely due to the presence of low levels of the putative receptor in normal mammary cells. Peptides 18-9 and 18-10 displayed similar affinity profiles for the cancer and control cells with 18-9 showing slightly better selectivity. Therefore, 18-9 was selected for subsequent experiments.

In a parallel experiment the binding specificity and cellular uptake of 18-4 and 18-9 peptides were studied using fluorescence microscopy in MDA-MB-435 and HUVEC cells. The fluorescently (FITC) labeled peptides were incubated with cells for 30 min at 37 °C and the peptide distribution was examined. Both the FITC-labeled peptides were found to be strongly bound to the cell membrane of MDA-MB-435 cancer cells and were also uniformly distributed inside the cells (Figure 3, left side). In contrast, the uptake of the peptides by control HUVEC cells was minimal under the same experimental conditions (Figure 3, right side). To further prove that most peptide molecules were not only surface bound but also internalized, we performed optical sectioning of MDA-MB-435

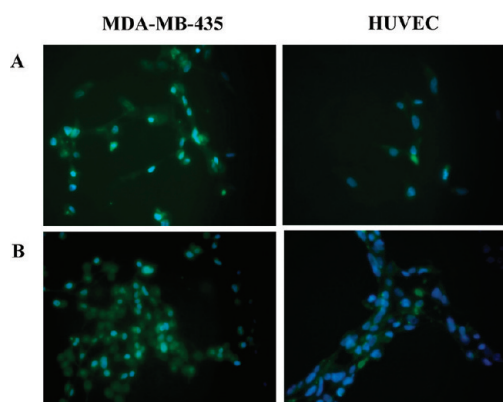


**Figure 3.** Fluorescence microscopy images of MDA-MB-435 and HUVEC cells after incubation with FITC-18-4 (A) or FITC-18-9 (B) for 30 min at a peptide concentration of  $10^{-5}$  mol/L. Cell nuclei were stained blue with DAPI.

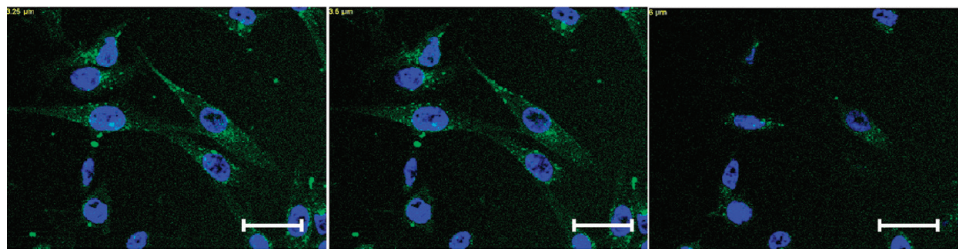
cells treated with 18-9 (Figure 4). The focal plane was changed from bottom to top in the vertical axis range of  $32.8 \mu\text{m}$  at an interval of  $1.64 \mu\text{m}$ , and as shown in Figure 4, it was found that most of the peptide bound to MDA-MB-435 cells was internalized by the cells.

The specificity of the peptides was evaluated by a competitive binding experiment. MDA-MB-435 cells were incubated with FITC-labeled peptides ( $10^{-5}$  mol/L) in the presence of a 50-fold excess of unlabeled 18-4 or 18-9 for 30 min, and fluorescence was measured using flow cytometry. Both peptides led to a substantial decrease in fluorescence when incubated with an excess of unlabeled peptide. Peptide 18-4 caused an up to 50% decrease in binding of the FITC-peptide, and 18-9 led to about a 40% decrease in binding, suggesting specific binding of the peptides to the cancer cells.

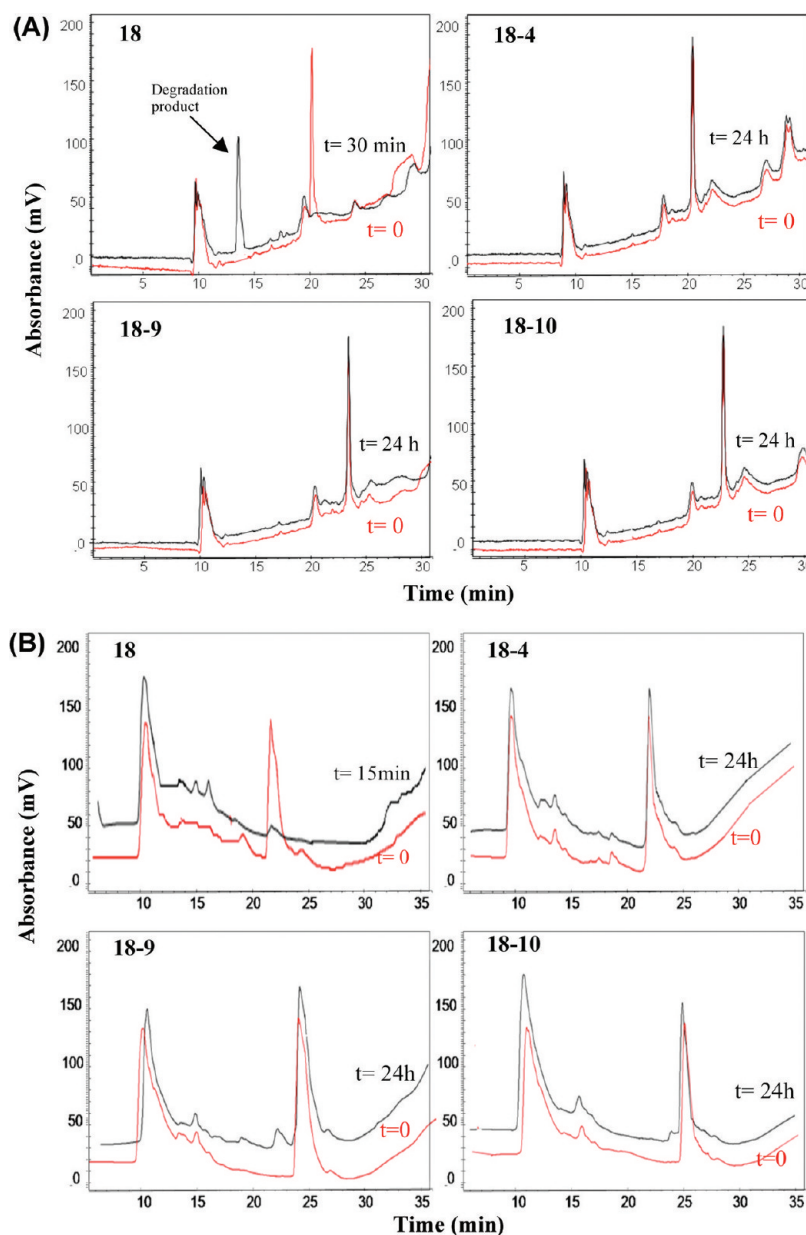
**Proteolytic Stability.** Next, the ability of these peptides (18-4, 18-9, and 18-10) to be recognized and processed by proteolytic enzymes was explored. Susceptibility to proteolytic digestion by human serum was compared to  $\alpha$ -peptide 18. Peptides were incubated with human serum at 37 °C, and aliquots were removed for analysis at different time points up to 24 h. Serum was used in high specific concentration (25% serum) to be rate limiting so that a control peptide is degraded within 10 min. Degradation products were separated by reversed-phase HPLC in order to facilitate characterization by mass spectrometry.

Figure 5A shows the HPLC chromatograms of serum incubated with peptides for 0 and 24 h. Peptide 18 was completely degraded within 30 min, giving two main degradation products that appear after 10 min of incubation with serum. The degradation products of peptide 18 show masses of 997.1 and 878.1 g/mol, which correspond to EAAAYQRFL and WXEAAYQ sequences, respectively. This was in accordance with previous serum stability studies done for the p160 peptide.<sup>18</sup> In contrast, peptides 18-4, 18-9, and 18-10 were stable for more than 24 h after incubation with human serum. Serum aliquots were taken at 0.5, 1, 5, and 24 h after incubation with the peptides, and the peptides were found to be 100% intact (Table S2).

Peptides were also exposed to the liver homogenate to evaluate proteolytic stability. Incubation of peptides 18-4, 18-9, and 18-10 with the homogenate up to 48 h did not result in any detectable degradation (Table S1 and Figure 5B). In contrast, under similar conditions the  $\alpha$ -peptide 18 was completely fragmented in 15 min. It was observed that proteolysis



**Figure 4.** Optical sectioning using confocal laser microscopy of MDA-MB-435 cells showing intracellular distribution of FITC-labeled peptide **18-9**. Cells were incubated with the peptide for 30 min at 37 °C prior to analysis. Scale bars: 20  $\mu$ m.



**Figure 5.** RP-HPLC chromatograms of peptides **18**, **18-4**, **18-9**, and **18-10** after incubation with the human serum (A) and the liver homogenate (B). Peptides were incubated with the human serum or liver homogenate from mice for different time intervals, namely, 0 h (red), 30 min (black), and 24 h (black), prior to HPLC analysis. Peptides elute around 21–25 min. Degradation products from peptide **18** appear around 14–18 min, and the remaining peaks are from the medium.

predominantly arises from the cleavage of the N-terminal amino acids, probably because of aminopeptidase activity. The degradation products for peptide **18** detected by HPLC were isolated and characterized by mass spectrometry. The main

degradation products with masses 868.2, 797.2, and 727.4 g/mol corresponded to the sequences AAYQRFL, AYQRFL, and YQRFL, respectively. These results reveal that introduction of D-amino acids or  $\beta^3$ -residues in the peptide sequences confers

substantial resistance to proteolytic degradation relative to their  $\alpha$ -peptide counterpart **18**. Such insertion of D- or  $\beta$ -amino acids in the peptide backbone tends to protect neighboring amide bonds from proteolytic cleavage.<sup>27,36</sup>

**Solution Conformation.** Peptide **18** was discovered by screening a library of peptides based on the sequence of lead peptide p160. In order to understand the structural basis for the increased binding to the cancer cells of **18** compared to p160, we evaluated the NMR solution structures of these two peptides. First the NMR structure of p160 was obtained in water and TFE. Peptide p160 was found to be helical in TFE; however, it displayed no regular secondary structure in water. An overlay of multiple structures of p160 in the two solvents showed that the peptide was more stabilized in TFE compared to water, demonstrated by the floppy N- and C-termini in the latter solvent (Figure 6 A). As these peptides are expected to

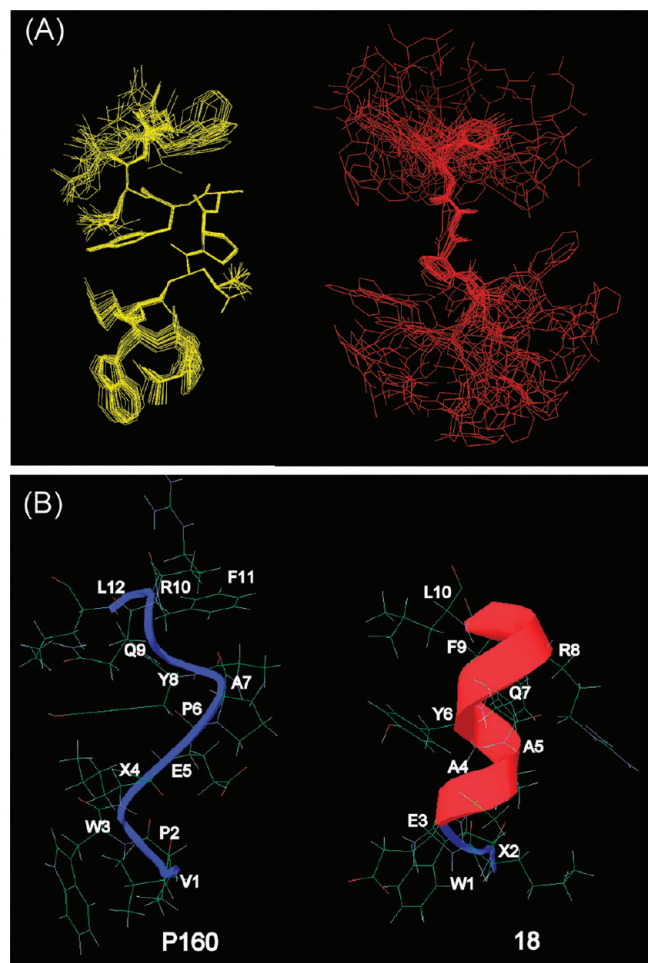


**Figure 6.** (A) NMR solution structures of peptide p160 in TFE (yellow) and water (red). (B) Comparison of the NMR structures of peptides p160 (LHS) and **18** (RHS) in TFE. The helical region in **18** extends from Glu3 (E3) to Phe9 (F9).

bind the cell surface during interaction with the cancer cells, TFE may be the more relevant solvent to study their solution conformation. Accordingly, we looked at the NMR structure of peptide **18** in 80% TFE and found that peptide **18** is more helical than p160 (Figure 6 B). In addition, peptide **18** presents three distinct faces, with aromatic residues W1, Y6, and F9 on one side, hydrophobic residues Nle2, A4, and A5 on another side, and polar residues Q7 and R8 on the third face. The

helical structure and the distinct binding faces could explain the stability of peptide **18** and increased affinity for the putative cancer cell surface receptor.

The solution conformation of peptide **18** and peptide analogues **18-4**, **18-9**, and **18-10** were compared using circular dichroism (CD) spectroscopy (Figure 7). The CD measurements

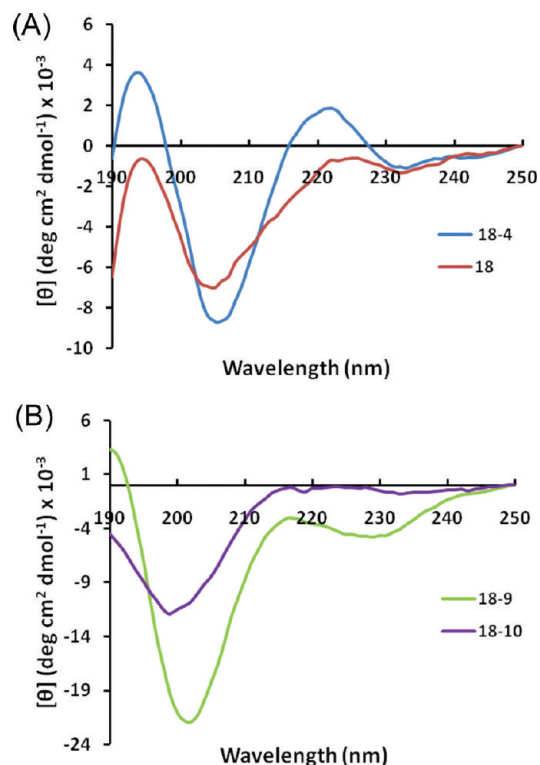


**Figure 7.** Circular dichroism spectra of peptides (A) **18** and **18-4** and (B) **18-9** and **18-10** in 90% TFE at 25 °C. The peptide concentration was 200  $\mu\text{M}$ .

were performed in 90% TFE/water at 200  $\mu\text{M}$ . Peptide **18** showed a strong minimum at 205 nm ( $\Theta = -7.0 \times 10^3$ ) with a shoulder at 231 nm. The minimum observed typically for helical peptides at 222 nm was not present. This is presumably due to diminished ellipticity at 222 nm in short helical peptides which consist of less than 5 turns.<sup>37,38</sup> Peptide analogue **18-4**, with Nle2 and Arg8 replaced with D-amino acids in the sequence of **18**, showed a CD spectrum similar to that of **18**, suggesting that the helical secondary structure is maintained. Interestingly, peptide **18-4** showed a slight increase in the molar ellipticity at 205 nm ( $\Theta = -8.7 \times 10^3$ ) and 195 nm ( $\Theta = 3.9 \times 10^3$ ) compared to peptide **18**. In this context, previous studies have shown that D-residues can indeed be comfortably accommodated in right-handed helix structures, as demonstrated by recent crystal structures of synthetic peptides containing multiple D-residues placed in host L-amino acid sequences.<sup>39,40</sup>

The CD spectra of mixed  $\alpha/\beta$ -peptides **18-9** and **18-10** showed marked difference from the spectra of  $\alpha$ -peptides. With three  $\beta$ -amino acids replacing three  $\alpha$ -residues in a 10-mer peptide, the CD spectra of **18-9** and **18-10** showed a minimum around 200–202 nm ( $-22 \times 10^3$  and  $-12 \times 10^3$ , respectively) and a small shoulder at 230 nm (Figure 7 B). CD spectra of several types of mixed  $\alpha/\beta$ -peptides have been reported and suggest that formation of a helix-like conformation is signaled by the strong minimum at 203–207 nm.  $\alpha/\beta$ -Peptides that do



not fold display little CD signal in this region.<sup>24,41</sup> This confirms our conjecture regarding the helical nature of **18-9** and **18-10**.

**Cytotoxicity.** Peptides **18-4**, **18-9**, and **18-10** were evaluated for their cytotoxic effects on MDA-MB-435 breast cancer cell line using the MTT assay. Doxorubicin (Dox) was used as a positive control. Different concentrations of the peptides and Dox were incubated with the cells, and after 48 h of incubation the percent cell viability was plotted as a function of the peptide concentration (Figure S6). The results showed that Dox displayed significant cytotoxicity with almost complete cell inhibition at 15  $\mu\text{M}$ . In contrast, all the tested peptides exhibited negligible toxicity on the cells with cell viability of  $>98 \pm 5\%$  at concentrations up to 100  $\mu\text{M}$ . This is consistent with our previous results that showed very low cytotoxicity of peptides synthesized from  $\beta^3$ -amino acids derived from L-Asp.<sup>25</sup> Dox displays toxicity in the nanomolar range against most cell lines; however, it shows relatively low toxicity against MDA-MB-435 cells, as observed here and elsewhere.<sup>42,43</sup>

## DISCUSSION

Chemotherapy and hormonal therapy play important roles in breast cancer treatment. Nevertheless, emergence of drug resistance and negative side effects of these therapeutic regimens necessitate the search for specific tumor targeting agents. The clinical success of monoclonal antibodies such as Herceptin, Zevalin, and Rituxan in the treatment of human cancer has validated the cell surface targeting approach in cancer therapy.<sup>44–46</sup> Peptides can be better cell surface targeting agents than antibodies, in particular when used as carriers for cytotoxic payloads such as chemotherapeutic agents or radionuclides. Peptides are smaller, safer, and more stable at room temperature with increased shelf life.<sup>47</sup> However, peptide applicability is limited because of fast proteolytic degradation. For instance, peptides p160 (shown previously)<sup>18</sup> and **18** display minimal stability in human serum, as they are completely degraded within 1 h after incubation with human serum (Figure 5). In addition, previous *in vivo* investigation of p160 stability in mice revealed a fast degradation of p160 in serum with appearance of degradation products after 2 min in circulation.<sup>18</sup> After *iv* administration, <sup>131</sup>I-labeled p160 showed higher uptake in tumors than in most normal organs but also showed elevated levels in the blood. This could be due to the interaction of p160 with serum proteins or the presence of degraded fragments that are unable to bind tumor and circulate in the bloodstream.<sup>18</sup>

Our objective in this study was to design proteolytically stable peptides with high specificity for cancer cells. The results show that we have designed and synthesized at least three peptide analogues derived from peptide **18** that are proteolytically stable and display increased affinity for breast cancer cells compared to peptide **18**. Peptide **18-4**, where two labile residues were replaced with D-amino acids, was completely stable in the presence of human serum and liver homogenate from mice (Figure 5) and showed up to 3.5-fold enhanced binding to cancer cells (Figure 2). Replacement of  $\alpha$ -residues with  $\beta$ -amino acids derived from L-Asp yielded two proteolytically stable peptides (**18-9** and **18-10**) with better binding profiles (2.8- to 3.1-fold) than peptide **18**. Interestingly, both these peptides include replacement of one residue each from the three distinct binding faces (aromatic, hydrophobic, and polar) identified in the NMR solution structure of peptide **18**. Replacement of W1, A4/A5, and R8 in peptide **18** with

$\beta$ -amino acids to yield **18-9** or **18-10** seems to align the side chains better for binding to cancer cells compared to substitutions in peptides **18-7** and **18-8**, where more than one residue has been replaced from a single binding face. Peptides **18-7** to **18-10** were designed to yield a stripe of  $\beta$  residues running along one side of the helix to stabilize secondary structure and increase receptor interaction. Such substitutions based on sequence based design strategy have generated different promising ligands.<sup>23,24,34</sup> The CD spectra suggest that peptides **18-9** and **18-10** are folded in solution (Figure 7); however, the exact nature of the fold will require elucidation of the three-dimensional structure. Like peptide **18**, which binds MDA-MB-435 cells with an apparent dissociation constant ( $K_d$ ) of 41.9  $\mu\text{M}$ ,<sup>19</sup> analogues **18-4** and **18-9** also recognize cancer cells with low micromolar affinity (data not shown).

It has now become clear that replacement of a few isolated  $\alpha$ -residues in an  $\alpha$ -peptide confers proteolytic stability.<sup>24,28</sup> In this study, replacement of two (**18-4**) or three residues (**18-9** and **18-10**) in a 10-mer peptide with D- or  $\beta^3$ -amino acids led to complete proteolytic stability (Figure 5). It is important to note that the  $\beta$ -amino acids used in this study are derived from L-Asp (Table 1) and are different from the  $\beta^3$ -amino acids synthesized from homologation of  $\alpha$ -residues.<sup>48,49</sup> The advantage of using  $\beta^3$ -amino acids derived from L-Asp is that they are readily synthesized during peptide assembly and are cheaper than the commercially available ones.<sup>29</sup> Further, the addition of  $\beta$ -amino acid side chain on the  $\alpha$ -carboxylate of L-Asp during peptide assembly allows introduction of a variety of unnatural side chains. This provides flexibility to control physicochemical properties of peptides and modulate binding affinity and selectivity.

Peptide sequences containing the amino acid sequences RGD or NGR have been widely used for tumor targeting and have made important contributions in the field of targeted drug delivery and medical imaging. These peptides have been shown to deliver a variety of cargo to cancer sites including cytotoxic drugs, cytokines, antiangiogenic compounds, viral particles, fluorescent compounds, contrast agents, DNA complexes, and other biologic response modifiers.<sup>50,51</sup> The RGD peptides target integrins such as  $\alpha v\beta 3$  and  $\alpha v\beta 5$ , whereas NGR binds CD13 (aminopeptidase N). Both integrins and CD13 are highly expressed on tumor vasculature. Recently Sugahara et al. showed that coadministration of a new generation RGD analogue, iRGD, improved the therapeutic index of various anticancer agents such as doxorubicin, nanoparticles carrying drug, and a monoclonal antibody trastuzumab. Chemical conjugation of iRGD to these entities was not required.<sup>52</sup>

Askoxyllakis et al. showed that radiolabeled p160 achieved better tumor targeting *in vivo* compared to RGD-4C. P160 and p160 derived peptides such as **18**, **18-4**, and **18-9** show high specificity for cancer cells (Figure 2), although the receptor for these peptides is not yet known. The plausibility of receptor mediated binding to the cancer cells is shown here by competition experiments (Figure S5) and also by Askoxyllakis et al.<sup>18</sup> These peptides are also internalized by the cells (Figures 3 and 4) and therefore can deliver drugs inside the cancer cells. Recently, we showed that p160-coated polymeric micelles display better binding and internalizing in MDA-MB-435 cells than c(RGDfk) micelles.<sup>53</sup> In addition, p160-decorated micelles showed better results over c(RGDfk) micelles with respect to selective cytotoxicity of encapsulated paclitaxel (PTX) against MDA-MB-435 cells over normal HUVEC and MCF10A cells. The better interaction of PTX nanocarriers with

cancer cells over normal cells achieved through p160 targeted ligand is expected to improve the biodistribution of the drug. Better homing of the drug into malignant cells and away from normal tissues can lead to better in vivo therapeutic index for the encapsulated PTX. This may also lead to a better penetration of the targeted drug carrier into the tumor mass. Consequently, peptides **18-4**, **18-9**, and **18-10** identified here could serve as better cancer targeting peptides, responding to the continuous demand for short peptide ligands for cancer specific diagnostic and therapeutic probes.

## CONCLUDING REMARKS

Three analogues of peptide **18** (**18-4**, **18-9**, and **18-10**) with high specific binding to breast cancer cell lines were discovered in the current investigation. These analogues exhibit resistance to proteolytic degradation and impart no cytotoxicity. These peptides have a high degree of secondary structure that correlates with their binding affinity and internalization. We envision our peptide analogues as useful, enzymatically stable lead peptides that can either directly couple to an anticancer drug, decorate a drug carrier that encapsulates the drug (e.g., liposomes, micelles, and polymeric nanoparticles), or conjugate with a diagnostic moiety such as a fluorophore or nonmetallic isotope. Targeted therapy using cancer targeting peptides restricts the toxic effect of a drug to the malignant tissues, thereby increasing the efficacy and decreasing the undesired side effects of the drug. Hence, the peptides reported here would serve as favorable candidates for use in cancer drug targeting or diagnosis. The strategy used to develop these breast cancer specific peptide analogues involved two steps. First, a synthetic library based on peptide p160, identified from phage display by Zhang et al.,<sup>16</sup> was screened for specific binding to breast cancer cells (done previously).<sup>19</sup> Second, analogues of peptide **18** identified from the above screening were engineered for proteolytic stability while maintaining high specificity for breast cancer cells. The stepwise procedure delineated here may be adapted for developing peptide analogues for targeting other cancer cell types.

## ASSOCIATED CONTENT

### Supporting Information

Tables S1–S3 and Figures S1–S6 related to peptide synthesis, characterization (HPLC and mass spectrometry), degradation, NMR structure elucidation, cytotoxicity, and uptake (flow cytometry). This material is available free of charge via the Internet at <http://pubs.acs.org>.

## AUTHOR INFORMATION

### Corresponding Author

\*Phone: 780-492-8917. Fax: 780-492-1217. E-mail: [kkaur@ualberta.ca](mailto:kkaur@ualberta.ca).

## ACKNOWLEDGMENTS

The authors thank Sahar Ahmed for assistance in the cell culture experiments and Elaine Moase for providing the liver homogenate. This work was supported by the Natural Sciences and Engineering Research Council of Canada (NSERC). The infrastructure support from the Canada Foundation for Innovation (CFI) is also acknowledged. NMR spectra were recorded at the Quebec/Eastern Canada High Field NMR Facility, supported by NSERC. R.S. is the recipient of the Egyptian Government Scholarship.

## ABBREVIATIONS USED

ACN, acetonitrile; L-Asp, L-aspartic acid; BCA, bicinchoninic acid protein assay; CD, circular dichroism; DAPI, 4',6-diamidino-2-phenylindole; DCM, dichloromethane; DIC, 1,3-diisopropylcarbodiimide; DIPEA, *N,N*-diisopropylethylamine; DMF, dimethylformamide; DMSO, dimethylsulfoxide; DOX, doxorubicin; Et<sub>2</sub>O, diethyl ether; FBS, fetal bovine serum; Fmoc, 9-fluorenylmethyloxycarbonyl; 5-FITC, fluorescein 5-isothiocyanate; HCTU, 2-(6-chloro-1*H*-benzotriazole-1-yl)-1,1,3,3-tetramethylammonium hexafluorophosphate; HEPES, 4-(2-hydroxyethyl)-1-piperazineethanesulfonic acid; HOBt, *N*-hydroxybenzotriazole; MALDI-TOF, matrix assisted laser desorption ionization time of flight; MTT, 3-(4,5-dimethylthiazol-2-yl)-2,5-diphenyltetrazolium bromide; NMR, nuclear magnetic resonance; NMM, *N*-methylmorpholine; PBS, phosphate buffered saline; RP-HPLC, reversed phase high performance liquid chromatography; TFA, trifluoroacetic acid; TFE, 2,2,2-trifluoroethanol; TIPS, triisopropylsilane

## REFERENCES

- (1) Takimoto, C. H.; Calvo, E. Principles of Oncologic Pharmacotherapy In *Cancer Management: A Multidisciplinary Approach*, 11th ed.; Pazdur, R., Wagman, L. D., Camphausen, K. A., Hoskins, W. J., Eds.; CMP: Manhasset, NY, 2008.
- (2) Abrous-Anane, S.; Savignoni, A.; Daveau, C.; Pierga, J.-Y.; Gautier, C.; Rey, F.; Dendale, R.; Campana, F.; Kirova, Y. M.; Fourquet, A.; Bollet, M. A. Management of Inflammatory Breast Cancer after Neoadjuvant Chemotherapy. *Int. J. Radiat. Oncol., Biol., Phys.* **2011**, *79*, 1055–1063.
- (3) Raschi, E.; Vasina, V.; Ursino, M. G.; Boriani, G.; Martoni, A.; De Ponti, F. Anticancer Drugs and Cardiotoxicity: Insights and Perspectives in the Era of Targeted Therapy. *Pharmacol. Ther.* **2010**, *125*, 196–218.
- (4) Bosslet, K.; Straub, R.; Blumrich, M.; Czech, J.; Gerken, M.; Sperker, B.; Kroemer, H. K.; Gesson, J.-P.; Koch, M.; Monneret, C. Elucidation of the Mechanism Enabling Tumor Selective Prodrug Monotherapy. *Cancer Res.* **1998**, *58*, 1195–1201.
- (5) Junutula, J. R.; Raab, H.; Clark, S.; Bhakta, S.; Leipold, D. D.; Weir, S.; Chen, Y.; Simpson, M.; Tsai, S. P.; Dennis, M. S.; Lu, Y.; Meng, Y. G.; Ng, C.; Yang, J.; Lee, C. C.; Duenas, E.; Gorrell, J.; Katta, V.; Kim, A.; McDorman, K.; Flagella, K.; Venook, R.; Ross, S.; Spencer, S. D.; Wong, W. L.; Lowman, H. B.; Vandlen, R.; Sliwkowski, M. X.; Scheller, R. H.; Polakis, P.; Mallet, W. Site-Specific Conjugation of a Cytotoxic Drug to an Antibody Improves the Therapeutic Index. *Nat. Biotechnol.* **2008**, *26*, 925–932.
- (6) Govindan, S. V.; Goldenberg, D. M. New Antibody Conjugates in Cancer Therapy. *TheScientificWorldJournal* **2010**, *10*, 2070–2089.
- (7) Aina, O. H.; Sroka, T. C.; Chen, M.-L.; Lam, K. S. Therapeutic Cancer Targeting Peptides. *Pept. Sci.* **2002**, *66*, 184–199.
- (8) Laakkonen, P.; Zhang, L.; Ruoslahti, E. Peptide Targeting of Tumor Lymph Vessels. *Ann. N.Y. Acad. Sci.* **2008**, *1131*, 37–43.
- (9) Lyakhov, I.; Zielinski, R.; Kuban, M.; Kramer-Marek, G.; Fisher, R.; Chertov, O.; Bindu, L.; Capala, J. HER2- and EGFR-Specific Affiprobe: Novel Recombinant Optical Probes for Cell Imaging. *ChemBioChem* **2010**, *11*, 345–350.
- (10) Eigenbrot, C.; Ultsch, M.; Dubnovitsky, A.; Abrahamsén, L.; Härd, T. Structural Basis for High-Affinity HER2 Receptor Binding by an Engineered Protein. *Proc. Natl. Acad. Sci. U.S.A.* **2010**, *107*, 15039–15044.
- (11) Shangguan, D.; Meng, L.; Cao, Z. C.; Xiao, Z.; Fang, X.; Li, Y.; Cardona, D.; Witek, R. P.; Liu, C.; Tan, W. Identification of Liver Cancer-Specific Aptamers Using Whole Live Cells. *Anal. Chem.* **2008**, *80*, 721–728.
- (12) Aina, O. H.; Liu, R.; Sutcliffe, J. L.; Marik, J.; Pan, C.-X.; Lam, K. S. From Combinatorial Chemistry to Cancer-Targeting Peptides. *Mol. Pharmaceutics* **2007**, *4*, 631–651.

- (13) Shukla, G. S.; Krag, D. N. Selection of Tumor-Targeting Agents on Freshly Excised Human Breast Tumors Using a Phage Display Library. *Oncol. Rep.* **2005**, *13* (4), 757–764.
- (14) Shadidi, M.; S. M. Selection of Peptides for Specific Delivery of Oligonucleotides into Cancer Cells. *Methods Mol. Biol.* **2004**, *252*, 569–580.
- (15) Shukla, G. S.; Krag, D. N. Novel  $\beta$ -Lactamase-Random Peptide Fusion Libraries for Phage Display Selection of Cancer Cell-Targeting Agents Suitable for Enzyme Prodrug Therapy. *J. Drug Targeting* **2010**, *18*, 115–124.
- (16) Zhang, J.; Spring, H.; Schwab, M. Neuroblastoma Tumor Cell-Binding Peptides Identified through Random Peptide Phage Display. *Cancer Lett.* **2001**, *171*, 153–164.
- (17) Askoxylakis, V.; Mier, W.; Zitzmann, S.; Ehemann, V.; Zhang, J.; Kramer, S.; Beck, C.; Schwab, M.; Eisenhut, M.; Haberkorn, U. Characterization and Development of a Peptide (p160) with Affinity for Neuroblastoma Cells. *J. Nucl. Med.* **2006**, *47*, 981–988.
- (18) Askoxylakis, V.; Zitzmann, S.; Mier, W.; Graham, K.; Krämer, S.; von Wegner, F.; Fink, R. H. A.; Schwab, M.; Eisenhut, M.; Haberkorn, U. Preclinical Evaluation of the Breast Cancer Cell-Binding Peptide, p160. *Clin. Cancer Res.* **2005**, *11*, 6705–6712.
- (19) Ahmed, S.; Mathews, A. S.; Byeon, N.; Lavasanifar, A.; Kaur, K. Peptide Arrays for Screening Cancer Specific Peptides. *Anal. Chem.* **2010**, *82*, 7533–7541.
- (20) Gorris, H. H.; Bade, S.; Röckendorf, N.; Albers, E.; Schmidt, M. A.; Fránek, M.; Frey, A. Rapid Profiling of Peptide Stability in Proteolytic Environments. *Anal. Chem.* **2009**, *81*, 1580–1586.
- (21) Adessi, C.; Soto, C. Converting a Peptide into a Drug: Strategies To Improve Stability and Bioavailability. *Curr. Med. Chem.* **2002**, *9* (9), 963–978.
- (22) Gentilucci, L.; De Marco, R.; Cerisoli, L. Chemical Modifications Designed To Improve Peptide Stability: Incorporation of Non-Natural Amino Acids, Pseudo-Peptide Bonds, and Cyclization. *Curr. Pharm. Des.* **2010**, *16*, 3185–3203.
- (23) Horne, W. S.; Price, J. L.; Keck, J. L.; Gellman, S. H. Helix Bundle Quaternary Structure from  $\alpha/\beta$ -Peptide Foldamers. *J. Am. Chem. Soc.* **2007**, *129*, 4178–4180.
- (24) Horne, W. S.; Johnson, L. M.; Ketas, T. J.; Klasse, P. J.; Lu, M.; Moore, J. P.; Gellman, S. H. Structural and Biological Mimicry of Protein Surface Recognition by  $\alpha/\beta$ -Peptide Foldamers. *Proc. Natl. Acad. Sci.* **2009**, *106*, 14751–14756.
- (25) Ahmed, S.; Kaur, K. The Proteolytic Stability and Cytotoxicity Studies of L-Aspartic Acid and L-Diaminopropionic Acid Derived  $\beta$ -Peptides and a Mixed  $\alpha/\beta$ -Peptide. *Chem. Biol. Drug Des.* **2009**, *73*, 545–552.
- (26) Frackenpohl, J.; Arvidsson, P. I.; Schreiber, J. V.; Seebach, D. The Outstanding Biological Stability of  $\beta$ - and  $\gamma$ -Peptides toward Proteolytic Enzymes: An in Vitro Investigation with Fifteen Peptidases. *ChemBioChem* **2001**, *2*, 445–455.
- (27) Hook, D. F.; Bindschädler, P.; Mahajan, Y. R.; Šebesta, R.; Kast, P.; Seebach, D. The Proteolytic Stability of “Designed”  $\beta$ -Peptides Containing  $\alpha$ -Peptide-Bond Mimics and of Mixed  $\alpha,\beta$ -Peptides: Application to the Construction of MHC-Binding Peptides. *Chem. Biodiversity* **2005**, *2*, 591–632.
- (28) Aguilar, M.-I.; Purcell, A. W.; Devi, R.; Lew, R.; Rossjohn, J.; Smith, A. I.; Perlmutter, P. [Small Beta]-Amino Acid-Containing Hybrid Peptides-New Opportunities in Peptidomimetics. *Org. Biomol. Chem.* **2007**, *5*, 2884–2890.
- (29) Ahmed, S.; Beleid, R.; Sprules, T.; Kaur, K. Solid-Phase Synthesis and CD Spectroscopic Investigations of Novel  $\beta$ -Peptides from L-Aspartic Acid and  $\beta$ -Amino-L-alanine. *Org. Lett.* **2006**, *9*, 25–28.
- (30) Kaiser, E. C. R.; Bossinger, C. D.; Cook, P. I. Color Test for Detection of Free Terminal Amino Groups in the Solid-Phase Synthesis of Peptides. *Anal. Biochem.* **1970**, *34*, 595–598.
- (31) Svenson, J.; Vergote, V.; Karstad, R.; Burvenich, C.; Svendsen, J. S.; De Spiegeleer, B. Metabolic Fate of Lactoferricin-Based Antimicrobial Peptides: Effect of Truncation and Incorporation of Amino Acid Analogs on the In Vitro Metabolic Stability. *J. Pharmacol. Exp. Ther.* **2010**, *332*, 1032–1039.
- (32) Güntert, P. Automated NMR Protein Structure Calculation with CYANA. *Methods Mol. Biol.* **2004**, *278*, 353–378.
- (33) van de Loosdrecht, A. A.; B. R., Ossenkoppele, G. J.; Broekhoven, M. G.; Langenhuijsen, M. M. A Tetrazolium-Based Colorimetric MTT Assay To Quantitate Human Monocyte Mediated Cytotoxicity against Leukemic Cells from Cell Lines and Patients with Acute Myeloid Leukemia. *J. Immunol. Methods* **1994**, *174*, 311–320.
- (34) Horne, W. S.; Boersma, M. D.; Windsor, M. A.; Gellman, S. H. Sequence-Based Design of  $\alpha/\beta$ -Peptide Foldamers That Mimic BH3 Domains. *Angew. Chem., Int. Ed.* **2008**, *47*, 2853–2856.
- (35) Schröder-Borm, H.; Bakalova, R.; Andrá, J. The NK-Lysin Derived Peptide NK-2 Preferentially Kills Cancer Cells with Increased Surface Levels of Negatively Charged Phosphatidylserine. *FEBS Lett.* **2005**, *579*, 6128–6134.
- (36) Horne, W. S.; Gellman, S. H. Foldamers with Heterogeneous Backbones. *Acc. Chem. Res.* **2008**, *41*, 1399–1408.
- (37) Aravinda, S.; Datta, S.; Shamala, N.; Balam, P. Hydrogen-Bond Lengths in Polypeptide Helices: No Evidence for Short Hydrogen Bonds. *Angew. Chem.* **2004**, *116*, 6896–6899.
- (38) Mahalakshmi, R.; Shanmugam, G.; Polavarapu, P. L.; Balam, P. Circular Dichroism of Designed Peptide Helices and  $\beta$ -Hairpins: Analysis of Trp- and Tyr-Rich Peptides. *ChemBioChem* **2005**, *6*, 2152–2158.
- (39) Aravinda, S. S. N.; Desiraju, S.; Balam, P. A Right Handed Peptide Helix Containing a Central Double D-Amino Acid Segment. *Chem. Commun.* **2002**, *20*, 2454–2455.
- (40) Karle, I. L.; Gopi, H. N.; Balam, P. Crystal Structure of a Hydrophobic 19-Residue Peptide Helix Containing Three Centrally Located D Amino Acids. *Proc. Natl. Acad. Sci. U.S.A.* **2003**, *100*, 13946–13951.
- (41) Sadowsky, J. D.; Fairlie, W. D.; Hadley, E. B.; Lee, H.-S.; Umezawa, N.; Nikolovska-Coleska, Z.; Wang, S.; Huang, D. C. S.; Tomita, Y.; Gellman, S. H. ( $\alpha/\beta$ )-Peptide Antagonists of BH3 Domain/Bcl-xL Recognition: Toward General Strategies for Foldamer-Based Inhibition of Protein–Protein Interactions. *J. Am. Chem. Soc.* **2006**, *129*, 139–154.
- (42) Serova, M.; Galmarini, C. M.; Ghoul, A.; Benhadji, K.; Green, S. R.; Chiao, J.; Faivre, S.; Cvitkovic, E.; Le Tourneau, C.; Calvo, F.; Raymond, E. Antiproliferative Effects of Sapacitabine (CYC682), a Novel 2[Prime]-Deoxycytidine-Derivative, in Human Cancer Cells. *Br. J. Cancer* **2007**, *97*, 628–636.
- (43) Teixeira, R.; Barbosa, L.; Maltha, C.; Rocha, M.; Bezerra, D.; Costa-Lotuf, L.; Pessoa, C.; Moraes, M. Synthesis and Cytotoxic Activity of Some 3-Benzyl-5-Arylidene-furan-2(SH)-ones. *Molecules* **2007**, *12*, 1101–1116.
- (44) Govindan, R. Cetuximab in Advanced Non-Small Cell Lung Cancer. *Clin. Cancer Res.* **2004**, *10*, 4241s–4244s.
- (45) Sandler, A. B.; Johnson, D. H.; Herbst, R. S. Anti-Vascular Endothelial Growth Factor Monoclonals in Non-Small Cell Lung Cancer. *Clin. Cancer Res.* **2004**, *10*, 4258s–4262s.
- (46) Albanell, J. A. J.; Baselga, J.; Codony-Servat, J.; Molina, M. A.; Rojo, F. Trastuzumab (Herceptin), a Humanized Anti-HER2 Receptor Monoclonal Antibody, Inhibits Basal and Activated HER2 Ectodomain Cleavage in Breast Cancer Cells. *Cancer Res.* **2001**, *61*, 4744–4749.
- (47) Shadidi, M.; Sioud, M. Selective Targeting of Cancer Cells Using Synthetic Peptides. *Drug Resist. Updates* **2003**, *6*, 363–371.
- (48) Cheng, R. P.; Gellman, S. H.; DeGrado, W. F.  $\beta$ -Peptides: From Structure to Function. *Chem. Rev.* **2001**, *101*, 3219–3232.
- (49) Seebach, D.; Gardiner, J.  $\beta$ -Peptidic Peptidomimetics. *Acc. Chem. Res.* **2008**, *41*, 1366–1375.
- (50) Auzzas, L.; Zanardi, F.; Battistini, L.; Burreddu, P.; Carta, P.; Rasso, G.; Curti, C.; Casiraghi, G. Targeting v3 Integrin: Design and Applications of Mono- and Multifunctional RGD-Based Peptides and Semipeptides. *Curr. Med. Chem.* **2010**, *17*, 1255–1299.
- (51) Wickström, M.; Larsson, R.; Nygren, P.; Gullbo, J. Amino-peptidase N (CD13) as a Target for Cancer Chemotherapy. *Cancer Sci.* **2011**, *102*, 501–508.

(52) Sugahara, K. N.; Teesalu, T.; Karmali, P. P.; Kotamraju, V. R.; Agemy, L.; Greenwald, D. R.; Ruoslahti, E. Coadministration of a Tumor-Penetrating Peptide Enhances the Efficacy of Cancer Drugs. *Science* **2010**, 328, 1031–1035.

(53) Shahin, M.; Ahmed, S.; Kaur, K.; Lavasanifar, A. Decoration of Polymeric Micelles with Cancer-Specific Peptide Ligands for Active Targeting of Paclitaxel. *Biomaterials* **2011**, 32, 5123–5133.